SATELLITE FLIGHT DYNAMICS ACTIVITIES SUPPORTED BY OPTICAL OBSERVATIONS, LESSONS LEARNT FROM OPERATIONAL EXPERIENCE

Noelia Sánchez-Ortiz(1), Raúl Domínguez-González(1), Jaime Nomen(1), Stefano Pessina(2), and Milan Klinc(3)

(1)Deimos Space, Ronda de Poniente 19, 28760, Tres Cantos, Madrid, 28760, Spain, Email: {noelia.sanchez, raul.dominguez, jaime.nomen}@deimos-space.com
(2)Eumetsat, Eumetsat Allee 1, 64295 Darmstadt, Germany, Email: Stefano.Pessina@eumetsat.int
(3)WGS Workgroup Solutions GmbH, Brüder Knauß Str. 6, 64285 Darmstadt, Germany, Email: Milan.Klinc@external.eumetsat.int

ABSTRACT

Since June 2018 EUMETSAT has incorporated SST like optical observations into the operational orbit determination process for the four geosynchronous Meteosat satellites, with the objective of assessing the suitability of optical data to support the operational activities, and evaluating the accuracy of routine orbit determination and manoeuvres calibration using mixed data from ranging stations and telescopes. Up to now, the flight dynamic activities were based on ranging data from a network of stations, with alternate tracking from two stations per satellite.

The optical measurements are provided by the Deimos Sky Survey (DeSS) telescopes, using additional sensors as a backup in case of adverse weather conditions or technical issues. The processing of the measurement data is performed by two separate teams at Eumetsat and Deimos.

Each satellite is observed at least twice per week, in routine mode, plus additional observations when required, for manoeuvre calibration purposes. The orbit determination based on those observations is automatically performed weekly by means of a Batch Least Squares approach with a two-week rolling window. In absence of manoeuvres, this allows determining the solar radiation pressure coefficient while maintaining consistency with the previously computed orbits. When a manoeuvre is scheduled, optical observations are taken as soon as possible after the manoeuvre itself. In this case, the paper shows that the orbit determination with optical information provides results comparable with the nominal range-only orbits, with accuracy gain in case of fusion of the different measurements. The paper describes some situations to be avoided where the manoeuvre calibration offers worse results, like the tracks collected with a time gap of about 24 hours.

This paper describes the processing chain put in place at Deimos for scheduling and performing the observations, and for the processing of measurement data, and it summarizes the findings after more than one year of service. The paper presents an evaluation of orbital quality and capability to estimate manoeuvres executed by the satellites, and identifies the benefits for satellite operators when using this novel approach for satellite operations based on this kind of observations.

Keywords: Optical; Telescope; Orbit Determination; Operational; Manoeuvre.

1. INTRODUCTION

Meteosat was initiated in 1972 as a meteorological program in GEO (Geostationary orbit) by the European Space Research Organization (ESRO), which was a predecessor organization to the European Space Agency (ESA). The first Meteosat satellite (Meteosat-1) was launched in 1977, with continous operations in GEO since then. The current entity that operates the Meteosat satellites is EUMETSAT (European Organisation for the Exploitation of Meteorological Satellites) formed as an international agency in 1986. In the present date, EUMETSAT is operating a fleet of 4 geostationary satellites, collectively referred to as Meteosat Second Generation (MSG). They are stationed over longitudes that allow them to cover the European mainland and the indian ocean area. In addition to the geostationary fleet, EUMETSAT is currently operating three LEO (Low Earth Orbit) satellites, with the objective of providing coverage to locations unreachable by the GEO fleet.

The MSG programme ground segment includes its service for orbit determination and control. This relies in the Mission Control Centre (Darmstadt, Germany), with ground stations currently located in Fucino (Italy) and Cheia (Romania) acting as the main points of communication with the satellites, and being used routinely for orbit determination. Additionally, a backup ground station is located in Maspalomas (Canary islands, Spain), and is used to provide ranging measurements in case of contingencies. These ground stations provide commu-

Proc. 8th European Conference on Space Debris (virtual), Darmstadt, Germany, 20–23 April 2021, published by the ESA Space Debris Office
Ed. T. Flohrer, S. Lemmens & F. Schmitz, (http://conference.sdo.esoc.esa.int, May 2021)

nications with the satellites, as well as two-way ranging measurements that are used for the operational orbit determination. This schema has changed recently. Before July 2019, the orbit determination was being performed regularly by the stations at Fucino and Maspalomas only.

Following several studies [3], [4], EUMETSAT has been complementing the primary orbit determination service with optical measurements since 2018. These measurements are provided by optical telescopes operated by Deimos Space located in Puertollano, Spain [1], [2]. These measurements are being used for routine orbit determination of the satellites, as well as for manoeuvre calibration. Its feasibility to complement the two-way ranging for future Meteosat satellites is currently under study [5].

In order for the ranging approach to provide adequate accuracies in orbit determination, it is necessary to ensure an adequate separation of the tracking stations [6]. Clearly, as the target satellites are geostationary, the observational geometry from ground based station is always very similar. In the case of ranging, this implies that uncertainties and biases in the observations are always located along the same direction. Clearly, combining observations from several locations helps removing these uncertainties from the solution. In the case of optical, the observed quantities are different (angles instead of ranges). In the case of optical, the same limitation (nearly constant geometry) exists, but the uncertanties are located in a plane perpendicular to the station-target line. [5] shows that the contribution of optical measurements improves the orbit determination results. Advantages of contributing optical measurements therefore include:

- Optical sensors are less costly than propietary ranging counterparts. Not only are they cheaper to operate, they can be also used for observation of other satellites.
- Optical observations are purely passive. Orbit determination can be performed even if the satellite transponder is in a non-functional state.
- Optical observations can be used to observe and determine the orbit of nearby objects. Objects with small relative velocity with respect to the target object can be observed for free, and this enables to perform independent threat assessment for these cases.
- These measurements are not affected by the ionosphere. Effects that need correction (refractions, aberrations) are well known.

The main drawbacks of the use of optical sensors are:

- Observations can be performed only in night time.
- There are other constraints: The satellite must be outside the shadow of Earth. Angular separation to the Moon and to the Milky Way (as well as the moon phase) impact on the measurement quality.

Satellite	IDs	EoL	Position	Service
Meteosat-11 (MSG4)	2015-034A	2033	0^o	FDS
Meteosat-10 (MSG3)	2012-035B	2030	9.5^o E	RSS
Meteosat-9 (MSG2)	2005-049B	2024	3.5^o E	RSS/backup
Meteosat-8 (MSG1)	2002-040B	2022	41.5^o E	IODC

Table 1. MSG fleet

- The optical sensor is sensitive to weather conditions.

The disadvantages can be overcome by deploying optical sensors with enough separation. In particular, locations should be chosen so that the weather in the different locations can be considered decoupled. Additionally, sites should be chosen considering the typical desireable conditions for optical observations (minimise light pollution, minimise yearly rainfall, ...)

1.1. Eumetsat geostationary fleet

The MSG satellites are spin-stabilized (100 rpm) satellites located in different locations in the GEO ring. They are drum-shaped (figure 1). The most relevant dimensions are 3.2 m in diameter and 3.7 m in height, of which 2.4 m correspond to the main body). They include an unified propulsion system (UPS) [7], with thrusters along the main axes for North-South Stationkeeping manoeuvres (NSSK) and thrusters tangent to the drum for other manoeuvres.

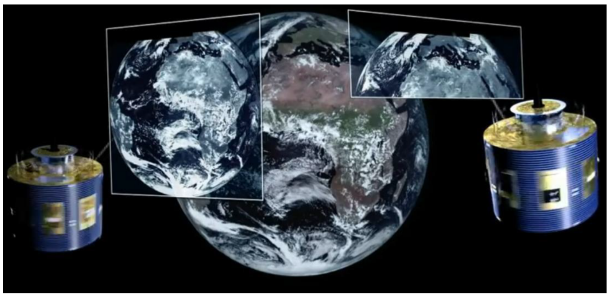

Figure 1. MSG satellites, Earth Full-Disk (left) and Rapid-Scan (right) services

They provide real time imagery of the Earth with Full-Disk Service (FDS, images every 15 minutes) and Rapid-Scan Service reduced areas (RSS, every 5 minutes) from geosynchronous orbit (see Table 1 and Figure 1), with additional support to Indian Ocean Data Coverage (IODC). The fleet has backup capabilities as well. All four satellites are observable from the Dess observatory (2), with continuous geometric visibility.

The satellites perform the following station-keeping manoeuvres as part of their nominal operations:

- NSSK: North-South Station Keeping manoeuvres.
- EWSK: East-West Station Keeping manoeuvres.

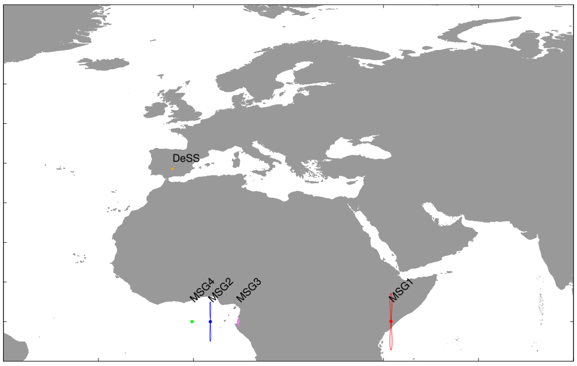

Figure 2. Groundtracks of EUM fleet and DeSS observatory location

- SLEW: For modifying the orientation.
- SPIN: Manoeuvre for modifying the satellite rotational speed.

1.2. DeSS

Deimos Sky Survey (DeSS) is an observatory owned and operated by Deimos Space. It comprises an observation site located in Puerto de Niefla, Castilla-La Mancha with four domes and a control centre located at the Deimos premises in Puertollano, Castilla-La Mancha. The sensors are controlled remotely from the control centre via a dedicated high speed radio link over a distance of 37 km, as seen in figure 4. The optical observation site location was chosen specifically so that there are no sources of light pollution in the vincinity. Additionally, the site was chosen attempting to maximize the number of usable observation nights (i.e, with adequate meteorological conditions) [8].

Figure 3. Annotated aerial view of the DeSS site (credit: Google)

Currently DeSS comprises four optical sensors: *Centu 1* for surveillance, *Tracker 1* and *Tracker 2* for tracking, and *Antsy* for tracking (including LEO tracking). The observatory is used daily to perform SST services for several customers. The *Tracker 2* sensor is dedicated to this activity (although, in case of need, the *Tracker 1* could perform the observations. Table 2 summarises the characteristics of this optical sensor (leftmost dome in Figure 4).

Optical design	Schmidt Cassegrain Coma-Free (ACF)
Aperture	400 mm
Focal length	3251 mm
Focal relation (f/R)	8 (5.5 with focal reducer)
FOV	21' x 21'
Resolution arcsec/pix	1.19
CCD chip	EMCCD 201 e2v Back-illuminated
CCD array	1024 x 1024
Pixel size microns	13 x 13
Quantum efficiency	90%
Colling temp	-95°

Table 2. Tracker 2 characteristics

Figure 4. DeSS observatory

Tracker 2 produces measurements with one 1-sigma accuracy of less than 1 arcsecond. In addition to this, all time bias is removed at sensor site. This time bias is determined by a means of routine calibration procedures, aimed at ensuring that the provided data does not drift away with time. Figure 5 shows an example of the noises found in a typical eumetsat track. It can be seen that no time-dependent behaviours can be observed. Also to be noticed is the small exposure time (less than 3 seconds), that allows reaching Signal-to-Noise ratios (SNR) of around 13.

Current developments in DeSS are aiming at compact and mobile optical ground stations, containing fully integrated systems for carrying out remote observations and processing of the images, including meteorological sensors, Uninterrupted Power Supply (UPS) and safe autonomous operations capabilities. These deployable systems are based on the small standard 2.4 meters cubic maritime containers.

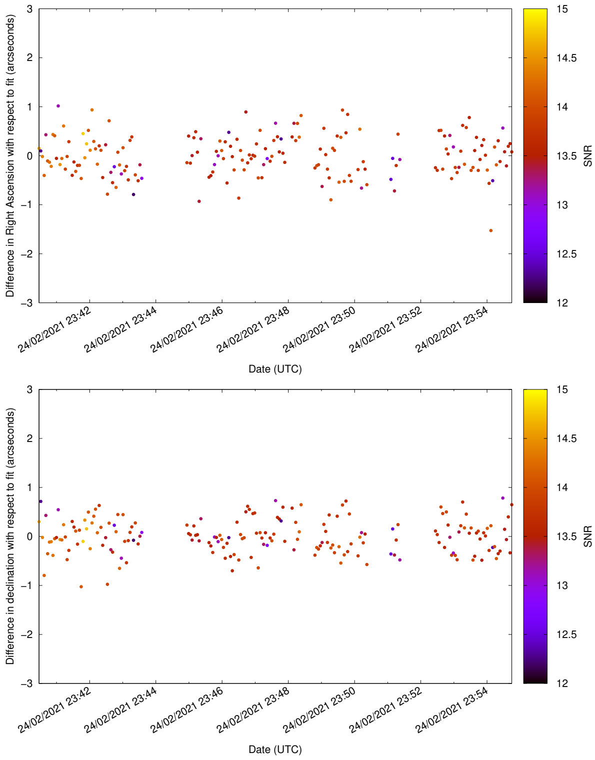

Figure 5. Differences in measured data with respect to polynomial fit ($R^2 = 0.999999$) for right ascension and declination measurements for a Tracker 2 *track*

2. DESCRIPTION OF THE SYSTEM

The central point of the Meteosat Second Generation ground segment is the Mission Control Centre (MCC) located at the Eumetsat premises (Darmstadt, Germany). From that location, communication with the satellite and retrieval of ranging data takes place through the antennae located in the Fucino (Italy) and Cheia (Romania) Primary Ground Stations (PGS), with a Backup Ground Station (BGS) located in Maspalomas, Canary Islands, Spain. This layout has changed slightly in the last years, with Cheia recently being promoted to primary location. Figure 6 details the locations of all entities.

The optical processing chain comprises the Deimos facilities. The control of the DeSS site takes place in the control Centre in Deimos Castilla-La Mancha. In case of need, it is possible to take control of the sensors from the premises in Madrid. In addition to the DeSS site, a backup site (Telescopi Joan Oró (TJO)), operated by the *Institut d'Estudis Espacials de Catalunya* (Institude of Space Studies of Catalonia). This backup site operates on an on-demand basis, when the weather forecast in the DeSS site make it impossibble to observe in the primary site.

The optical service is devised as an add-on to the range-based orbit determination. The most relevant highlights of the service are:

- At least, two observation slots per week and satellites.
- Each observation slot must comprise at least 15 minutes of observations.
- Slots must be separated by at least two hours.
- In case of satellite manoeuvre, a slot must be provided in the next 24 hours after the manoeuvre date

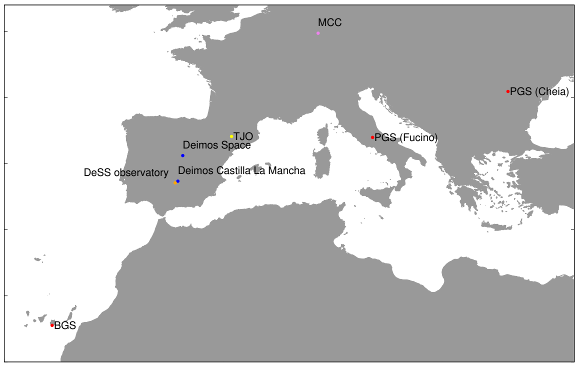

Figure 6. Components of the Eumetstat ground segment and additional optical service facilities

3. OPTICAL OBSERVATIONS

3.1. Telescope control

ITOX is a software tool developed at Deimos for supporting the remote control of optical sensors through the dedicated radio link. It controls the dome, sensor mount, CCD camera, dew removers, focusing, auto-synchronization, slewing, guiding, and the execution of all the observing sequences, including the timestamping of observations with accuracies under the millisecond. It allows to evaluate in real time the observability of satellites, and allows setting priorities. This tool includes a hardware-dependent layer, as all the aforementioned hardware items are tightly integrated in the program view. Figure 7

The tool is managed by an operator. Even though it would be possible to perform the operations in a fully automated way, it is risky to perform fully automated operations. In case of extremely good forecasts, fully automated operations can work with no issues. But, in case of not so good forecasts, when weather conditions change during the night, the system makes use of its automated routines for cancelling observations and closing domes automatically in case of dense clouds, rain, strong winds and high

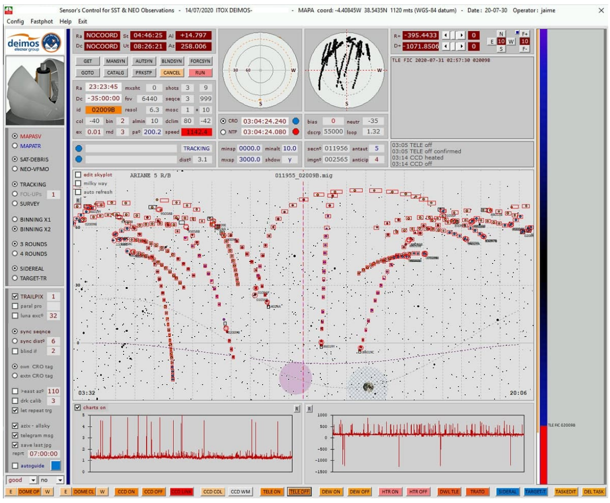

Figure 7. ITOX main view

humidity. With this, the sensor hardware is protected against potentially harmful weather conditions. The operator may override this if necessary. In general, observatories that rely on fully automated observations procedures are very conservative with respect to weather conditions for the reason of protecting the hardware. Additionally, in nights when the observation conditions are not optimal, the operator may choose to rearrange the observation plan on the fly, considering the priorities of different tasks, the remaining time, the presence of clouds in different parts of the sky, and many other factors.

Overall, the operator needs to continually assess when the conditions seem appropriate for running observations and this tool allows him/her to fully control all the aspects of the operation. The control system is complemented by an array of sensors that allow the operator to observe the conditions at the site (Figure 8).

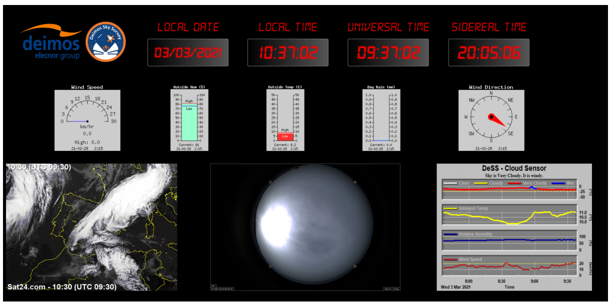

Figure 8. DeSS weather monitoring sensors dashboard

The environmental sensors include:

- Thermometers
- Humidity sensors
- Anemometer
- Rain sensor
- All-sky camera

Additionally, the weather forecast and evolution of cloud provided by weather providers is monitored as part of the operations.

3.2. Telescope processing

Images are obtained as a raw file (FITS: Flexible Image Transport System) which contain the lossless image, as well as metatada. ITOX adds metadata to each image in order to allow its processing and sorting by the TRAX tool. TRAX implements an algorithm for extracting and obtaining astrometry of moving objects (i.e, moving against the stars background). It requires a set of individual detections taken in a row (usually, three individual decections). This step removes false positives that can be caused by hot pixels or similar cases (as it is extremely unlikely that false detections appear in three sequential images with an apparent motion compatible with one of a satellite. This software is able to produce astrometry for both surveillance (where the satellites that will be observed are unknown) and tracking (where the expected position and trajectory of the satellite is an input to the process). In the case of the Eumetsat optical service, these trajectories are known a priori. Thanks to the metatada inserted by TRAX, the processing can better filter the observations by the expected angle of displacement and speed, as they are known from the nominal trajectory of the tracked satellite, thus filtering out false detections or other satellites appearing in the field of view. Figure 9 shows the main view of the tool, included three detections.

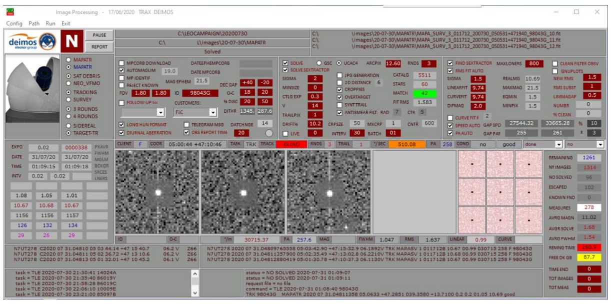

Figure 9. TRAX main view

This tool generates astrometry in the propietary HUN format. This format is based on the widely used at the Minor Planet Center (MPC), customized for observation of Earth Orbiting objects. The next picture displays an example of this format. It contains an identifier, the date down to the millisecond, measurements in topocentric right ascension and declination, visual magnitude, signal-to-noise ratio and angular speed.

```
ABOU001 2018 11 24.76404106460 23:18:30.30 -06:21:56.8 14.0535V TRK \
                    TRCKR2 1 3965604 15.74 00.68 000903 088 E 12035B
ABOU001 2018 11 24.76405700832 23:18:31.73 -06:21:55.1 14.1639V TRK \
                    TRCKR2 1 3965605 15.81 00.68 000903 088 E 12035B
ABOU001 2018 11 24.76407226970 23:18:33.02 -06:21:55.1 13.9356V TRK \
                    TRCKR2 1 3965606 15.76 00.68 000903 088 E 12035B
ABOU002 2018 11 24.76408748931 23:18:34.34 -06:21:55.3 14.0603V TRK \
                    TRCKR2 1 3965607 16.04 00.42 000896 089 E 12035B
ABOU002 2018 11 24.76410417823 23:18:35.78 -06:21:54.2 14.0352V TRK \
                    TRCKR2 1 3965608 15.92 00.42 000896 089 E 12035B
ABOU002 2018 11 24.76411858000 23:18:37.03 -06:21:54.4 14.1096V TRK \
                    TRCKR2 1 3965609 16.07 00.42 000896 089 E 12035B
```

Figure 10. Example of HUN format (lines have been split due to editorial reasons)

4. DESCRIPTION OF THE PROCESSING CHAIN

Eumetsat MCC and the optical service provider exchange the following items:

- Nominal orbits (from Eumetsat to Service provider)
- Manoeuvre plan (from Eumetsat to service provider)
- Optical observations (from service provider to Eumetsat)
- Orbits determined from optical data (from service provider to Eumetsat)
- Manoeuvre calibration report (from service provider to Eumetsat)

Within the optical service, weekly observations are scheduled considering the service requirements and the weather forecast. In case of favorable weather forecasts, weekly observations are widely spaced, while, in the case of unfavourable weather, the observations are taken as soon as possible. In the worst cases (very cloudy and/or rainy nights), the telescope operators monitor the weather conditions in real time, and perform observations when there is an opportunity (often, this means small opportunities in an otherwise cloudy night).

The processing chain is responsible of acting as interface between Deimos and Eumetsat and to perform orbit determination based on the optical products obtained by the Deimos Tracker 2 sensor, and the secondary sensors (whenever required). The interface functionality involves taking care of several different data fluxes. The processing chain itself is deployed in a single Linux machine. An additional secure FTP server in the Deimos infrastructure is set up, with data exchange happening automatically there by means of file exchange. The data storage is set up in a sqlite database and a dedicated storage folder. All the automated processes make use the database and the storage, and backups are taken regularly. The most relevant information that is stored includes:

- Definition of the Eumetsat GEO fleet, including all the relevant details required for observations and orbit determination.
- Optical sensors information (location, typical noise in measurements, known biases and whether they provide tracks corrected by annual aberration).
- Nominal manoeuvres provided by Eumetsat (start and end time, Delta-V and direction).
- Track files generated by the system (file metadata is stored in the database, and the files themselves are stored in the storage folder). Included raw astrometry (HUN format, as per 10)
- Incoming and outgoing OEM files (file metadata is stored in the database, and the files themselves are stored in the storage folder).

The system works with scheduled approach, with several data fluxes entering and leaving the system. Figure 11 shows the outbound fluxes and figure 12 shows the inbound fluxes.

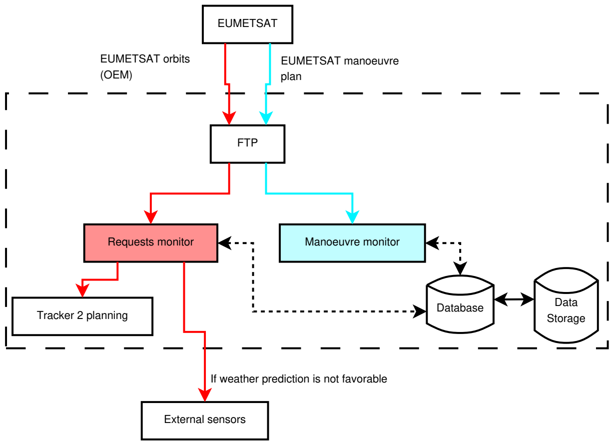

Figure 11. Inbound data fluxes managed by the processing chain

This processing chain was described in previous works ([1], [2]). In this work we describe the processing chain as it has undergone minor changes since the release of previous works.

4.1. Observations planning

The objective of this flux is to retrieve the primary operational orbits from Eumetsat, in order to use them for the optical sensor planning and pointing. These orbits always include the predicted manoeuvre. Observations planning is depicted as the red path in figure 11. The *Requests monitor* process polls the FTP for new orbits uploaded by Eumetsat. Whenever a new orbit is found, it is registered in the database and automatically copied to the Tracker 2 planning machine. In addition to this, an email is sent to the Deimos operators, with the file itself attached. This information is retrieved once per week.

Nominally, we plan observations at the beginning of the week, including primary slots and backup slots (in order to cover possible problems related to bad weather or unpredictable issues). In weeks when the weather forecast is not good, observations are attempted during the night when an opportunity arises. This means that the operator is monitoring the weather conditions continously and taking the chance to observe the targets whenever possible.

4.2. Manoeuvre processing

This data flux is implemented by the *Manoeuvre monitor* process. It receives the scheduled manoeuvre plan from Eumetsat and processes it, so other systems have its information available. In particular, the date of the manoeuvre and the nominal Delta-V are processed. This action is depicted as the cyan path in figure 11. The optical processing needs to take into account the manoeuvres performed by the satellites for the orbital determination process. For the routine orbit determination, which is performed by means of a Batch Least Squares (BLS) algorithm, the system selects the batches ensuring that no manoeuvre happens within a batch.

4.3. Track submission

Tracks meeting the conditions mentioned in section 2 are made available to Eumetsat once per week through the shared FTP in a batch. In addition to this, each individual track is made available the morning after it was taken, These processes are depicted as the green path in figure 12.

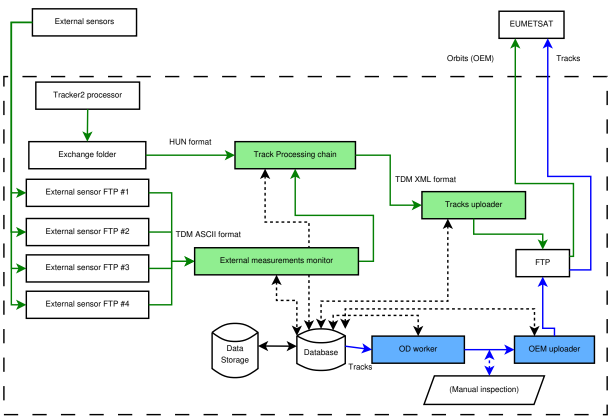

Figure 12. Outbound data fluxes managed by the processing chain

The main track processing is performed by the *Track processing chain*. It polls for tracks generated by the Tracker 2 sensor or made available by *External measurements monitor*. In the case of Tracker 2, there is a single HUN file per night, which contains all the observations performed by Tracker 2 in that particular night (see Figure 10)

This processing chain performs these actions:

1. Filter the HUN file, keeping only the observations tagged for Eumetsat.
2. Split the remaining measurements into groups, each group corresponding to a different observations slot.
3. Remove intruders in the groups. Intruders are observations of secondary objects that happen to be in the same field of view of the target object at the time of observation. This is performed with the TRACA tool (described in section 4.5).
4. Apply corrections to the tracks that require it. As each sensor provides tracks with different corrections applied, we make all the tracks homogeneous at this stage.
5. Apply time biases to sensors that require it.
6. Convert the remaining tracks into the TDM XML.
7. Register the tracks in the database and store them in the data storage.

Finally, the *Track uploader* is executed upon schedule. When it is executed, it verifies the database, checking for new files to be submitted. When there are new files to be submitted, and the agreed timeliness conditions are met, the files are uploaded to the FTP, and thus made available to Eumetsat, as well as registered as already uploaded in the database. When the daily uploads are performed, an automatic email is sent to the Deimos operator. Figure 13 shows an example of the information that is forwarded. For the weekly deliveries, the same information is provided for each of the files comprising the weekly batch. In addition to this, a summary of the total observation time and measurements for each of the satellites in the constellation is provided. In this case, the automatic email is sent to both the Deimos and Eumetsat operators.

```
File: FUCPGSA3_OPE_TDM_MSG1_20181014T082025_20181013T220035\
                                        _20181013T221724.tdm
MD5: af6b6039c86a3d2d4aac66d2fe62b44f
Target: MSG1 [METEOSAT-8 (MSG-1)]
Sensor: TRCKR2
Slot duration: 2018-10-13 22:00:35 - 2018-10-13 22:17:24 \
                               (16 minutes 49.0 seconds)
Number of measurements: 1212
Measurement rate: 1.20118929633 measurements/second
```

Figure 13. Example of data sent for individual track files (long lines have been edited)

4.4. Orbit determination

Orbit determination is performed daily with the optical tracks, and the results are made available in a weekly basis. The process is shown in figure 12, in blue. The *OD worker* retrieves from the database all the optical tracks within two weeks before the execution date. In case there is a manoeuvre within that period, only the tracks after the manoeuvre are considered for the Orbit Determination batch. Then, the TRADE tool (described in section 4.6) is executed. This tool performs the orbit determination and generates an OEM file with the determined orbit. Finally, the resulting orbit is compared with the orbit that was obtained the previous week. The result of the comparison is sent as well as part of the data delivery.

As mentioned before, the *OD worker* task is executed daily for each of the satellites and the results provided by it submitted once per week. This is achieved by the *OEM uploader*. This process just uploads the latest orbits and comparisons computed by the system to the FTP and registers them in the database. There is a time window between the execution of *OD worker* and *OEM uploader*. During that time window, the Deimos operators can manually check the orbit determination results. The system allows the operators to re-execute the TRADE tool, replacing the results of the manual execution. This design was devised in order to allow manually repeating the orbit determination in case some problem arises, while working fully automatically. Generally, the operators do not need to perform any action, and therefore, when the time window expires, *OEM uploader* uploads the orbits without further action. Upon uploading the orbits, an automatic email is issued with information about the computed orbits. Subsequent sections devoted to the orbit determination contain several examples of the data present in that email.

4.5. TRACA

TRACA is a tool meant to determine if individual optical observations can be assigned to the same physical Earth orbiting object. To do so, it implements an algorithm that attempts to build tracks with individual measurements, considering their compatibility. In order to check the compatibility, the apparent motion of the candidate tracks is considered (this is, the apparent motion is required to be smooth), as well as the compatibility of the apparent motion with an Earth orbit.

Figure 14 presents an example of the task performed by TRACA. The individual observations depicted in the figure were taken independently by the system. This is, each measurement was taken without making use of any information of previous measurements. An intruder object (red points) appeared in the sensor field of view during the slot time. Moreover, this intruder appears intermittently. This suggests that the intruder is spinning, and is probably a smaller object. In this case, TRACA is able to discern the two objects, because even though their individual measurements are all very similar, the apparent motions are not compatible. TRACA splits the observations into two tracks. Within the frame of this activity we discard the track related to the intruder, but in other SST related activities, intruder tracks are usually kept, as they correspond to real objects, and can be therefore relevant information for an SST system.

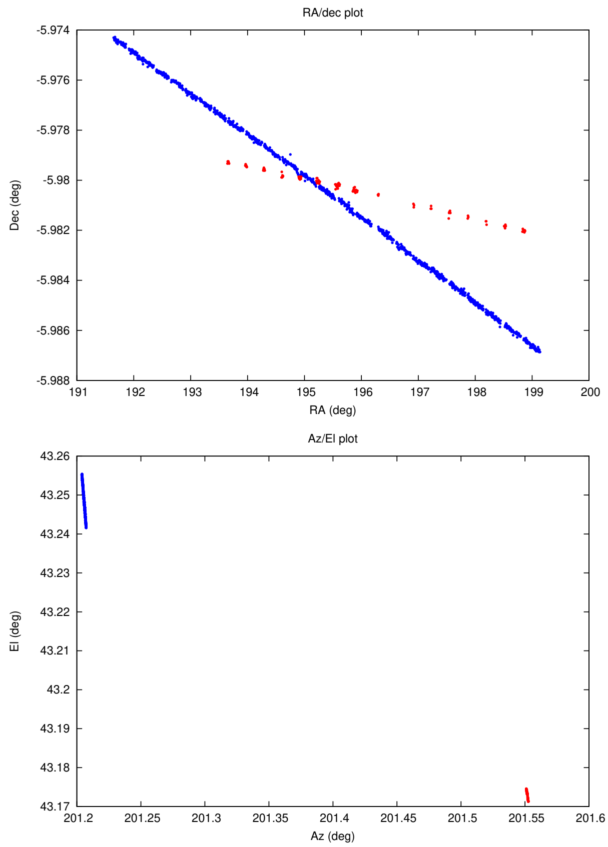

Figure 14. Example track separation performed by TRACA

4.6. TRADE

TRADE is a tool developed by Deimos focused for performing offline orbit determination with different algorithms. It implements an Square Root Information Filter (SRIF) [9] and Batch Least Squares (BLS) and Bayes filter [10]. TRADE supports optical telescopes and monostatic radars. In this context, we use a customized TRADE version with capabilities specific to the Eumetsat ranging data and to determine additional parameters. It is capable of processing tracks from different sensors (and of different types) simultaneously. It includes a numerical propagator with a detailed set of perturbations: Non-spheric Earth, third bodies, solar radiation pressure (SRP), atmoshpheric drag, albedo effect and solid tides. These perturbations are toggleable. It allows determining the orbital elements, the drag and solar radiation pressure coefficients, as well as the transponder delay at the satellite (part of the time budget in the two-way ranging measurements) .

TRADE computes the adjusted orbit at the epoch of the first measurement in the batch or at an user-defined epoch. It allows providing an initial estimation of the solution by means of TLEs, by interpolating over an user-provided OEM file or by manually inserting the value. It also implements initial orbit determination (IOD) algorithms for telescope and monostatic radars, so it is possible to obtain solutions without initial estimations (as long as the input data allows for a good IOD). As outputs, it provides per-sensor plots of the estimated residuals, as well as plots of the optical measurements in Right Ascension/Declination and Azimuth/Elevation. It also provides standard-compliant OEM orbits with or without covariances. Finally, it has the possibility of computing pointing opportunities for the determined orbits and the configured sensors network. The version used in this activity also includes the possibility of calibrating manoeuvres, this implementation is described with detail in section 5.2.

5. ACHIEVABLE QUALITIES AND PRODUCTS

In this section, we analyse the products generated during the service, focusing on the study of aggregated results during the operations.

5.1. Orbit determination with no manouvre

When no manoeuvre is scheduled, weekly data deliveries include an orbit determined using a 2-week batch time span (the orbit is computed making use of TRADE (described in 4.6). As observation nights do not happen at the same nights, this implies that not all orbit determinations involve 2 weeks exactly. Instead, it means that at most 2 weeks spans are used. In case manoeuvres happen, the orbit is determined only taking the latest observations after a manoeuvre. This approach ensures that the orbit can be determined without including the manoeuvre, but, on the other hand, implies that, after the manoeuvre, determined orbits will have lower accuracy because of the use of less data. This is acceptable, and additionally provides insight on how much time it is required to recover the orbit determination after a manoeuvre.

In addition to this, a comparison between the orbit that was determined last week and the currently determined orbit is attached to the delivery. This comparisons spans 7 days from the epoch of the last orbit determination (see figure 15). The comparison compares In the absence of higher quality reference data to compare to, this allows us to ensure that the determined orbits are consistent with each other. In the case of manoeuvres, this comparison is still performed even if it is not correct.

Figure 16 presents an example of the plots attached to the data delivery.

These comparisons have been performed every day since the beginning of the service. We can evaluate the long-term performance of the service by aggregating the data from all these comparisons.

In the first place, figures 17, 18, 19, and 20 present the average difference in position between each orbit and the

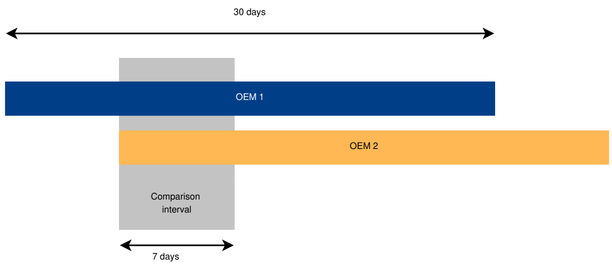

Figure 15. Definition of weekly orbit comparison rolling window

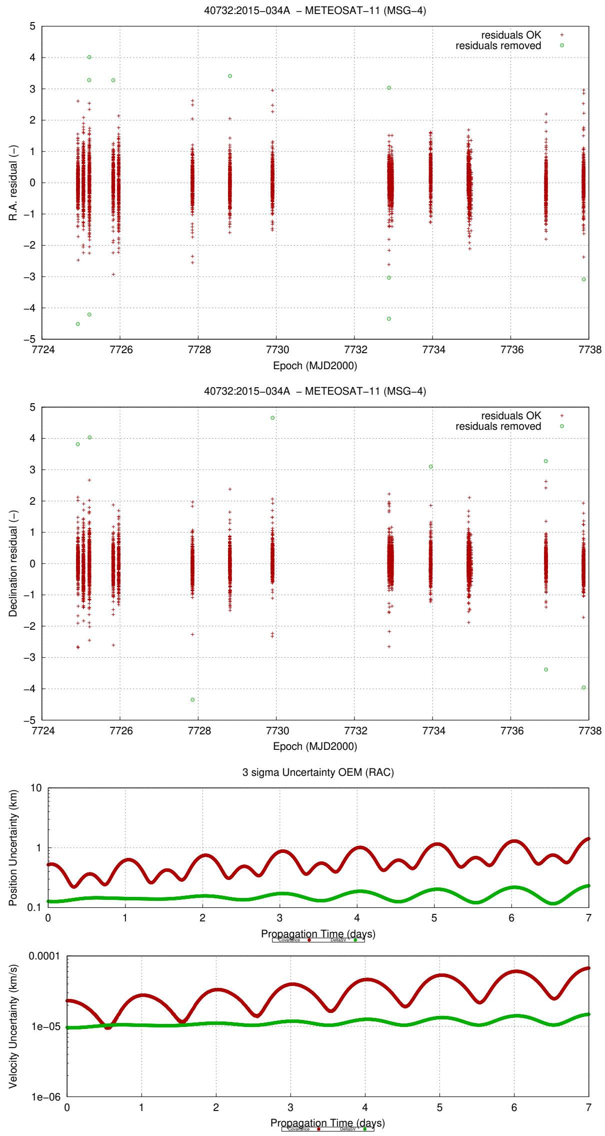

Figure 16. Example of orbit delivery items (MSG4 on 09/03/2021)

previous week for satellite MSG1. Manoeuvres were performed at the epochs depicted with vertical lines. It can be seen that the artificially bad qualities happen strictly after the manoeuvres (as explained above). For orbits not affected by manoeuvres, we can see that the differences in along-track stay well below 1 km, while the differences in cross-track and radial components are consistently one order of magnitude lower. The largest component of the error is always in the along-track component, as expectable.

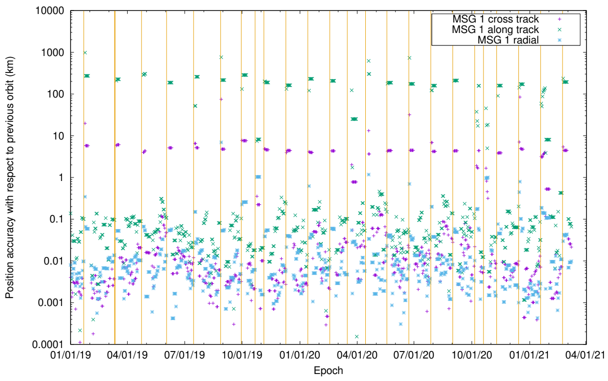

Figure 17. MSG1 comparison of each orbit determination against previous reference

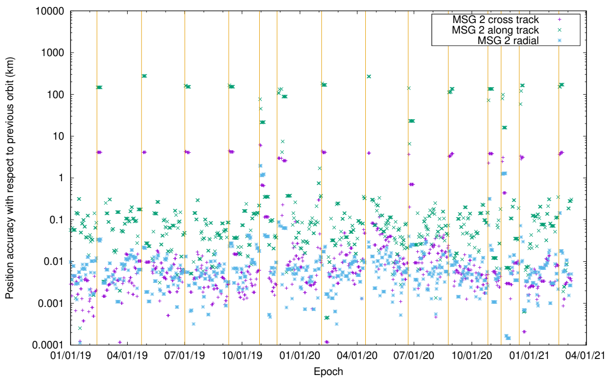

Figure 18. MSG2 comparison of each orbit determination against previous reference

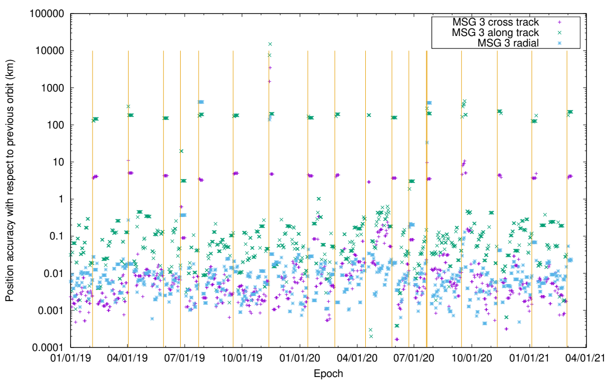

Figure 19. MSG3 comparison of each orbit determination against previous reference

The previous figures show that the solutions are consistent with each other, but are no use to verify the correctness of the solutions. For this, a comparison with independently generated data is necessary. Figures 21, 22, 23

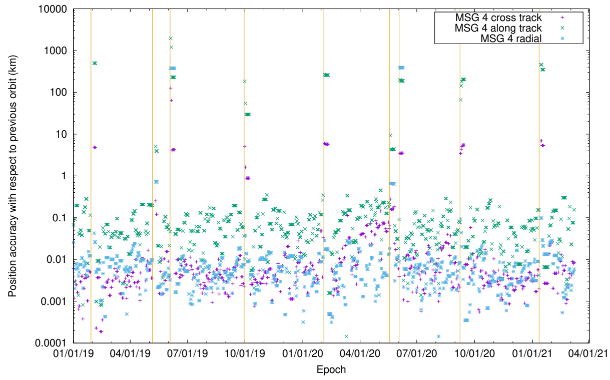

Figure 20. MSG4 comparison of each orbit determination against previous reference

and 24 show the comparison of the optical orbits against the orbits obtained from the ranging station data. In this case, the comparison is done in a 24 hour arc, and the maximum and minimum differences are displayed. There are some visible outliers, mainly after manoeuvres.

The main features that can be observed in these figures are:

- Outliers are caused by artifacts in the comparison when manoeuvres are performed.
- Differences in cross-track and radial components are centered in zero. This shows there is no bias between those components.
- There is a general tendency to a slightly biased result in the along-track component. This was found out to be mainly the result of a systematic error on Eumetsat flight dynamics. The fix for this issue is currently being tested, and will be deployed soon, therefore, future versions of this plot will have this bias removed.
- Starting from July 2019, the cross-track comparison of MSG3 and MSG4 becomes noticeable worse. Even though they are zero-centered, the magnitude of the difference increases sharply. The reason for this behaviour is that, as explained in section 1, at that time the nominal ground station locations were replaced. It went from Fucino + Maspalomas to Fucino + Cheia. This results in simular observational geometries, and therefore, a slightly worse cross-track accuracy. This is worse for the zero-inclination satellites. As MSG1 and MSG2 have a relevant inclination, this results in more varied observation geometries and thus the issue is mitigated. The new pair of ground locations have a smaller separation than the former. When the relocation was being planned, it was noticed and assumed that this slight loss of quality would happen.

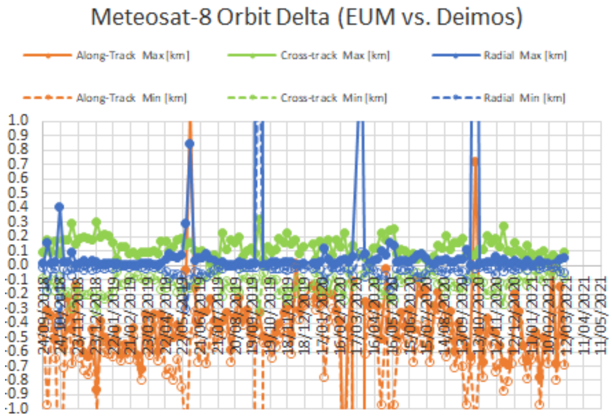

Figure 21. Comparison of MSG1 optical ephemeris against ranging orbits

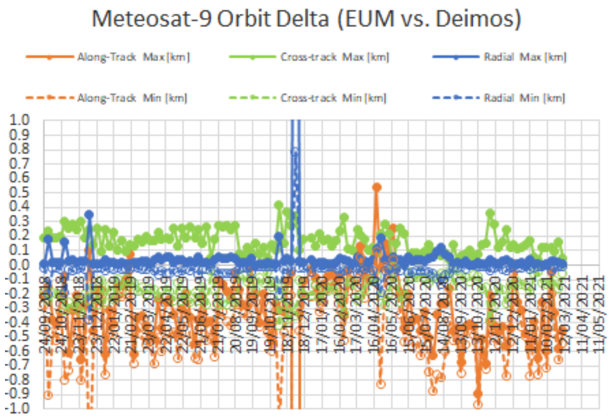

Figure 22. Comparison of MSG2 optical ephemeris against ranging orbits

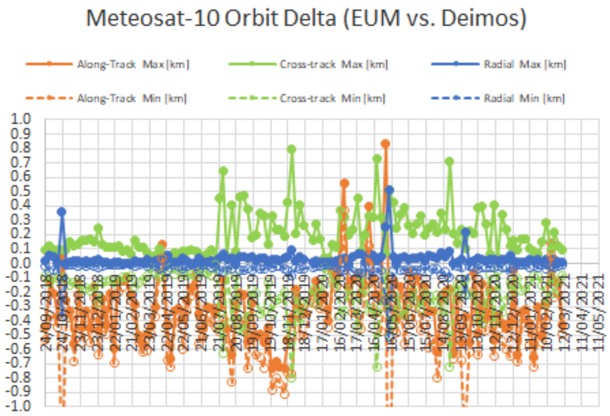

Figure 23. Comparison of MSG3 optical ephemeris against ranging orbits

5.2. Manoeuvre calibration

Manoeuvres performed by the GEO Eumetsat fleet were of types NSSK, EWSK and SLEW (see section 1.1 for a

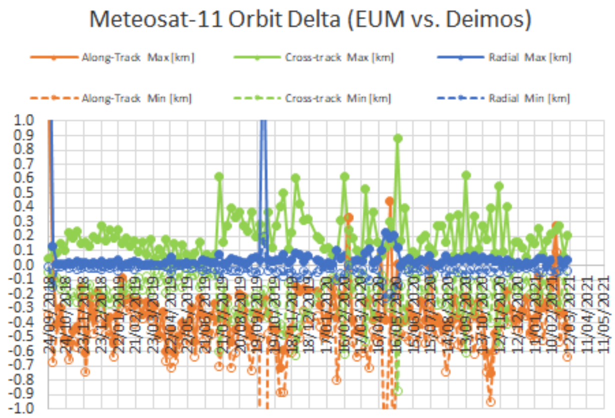

Figure 24. Comparison of MSG4 optical ephemeris against ranging orbits

complete list of possible manoeuvre types). NSSK manoeuvres are usually high magnitude ones, and are performed by the along-axis engine during a firing that usually takes a few minutes. EWSK and SLEW ΔVs are applied in the orbit plane by the manoeuvre engines. These engines are mounted tangentially to the main body, in pairs, so that, when a pair of engines is fired, the resultant thrust is directed through the center of mass of the satellite. As the satellites nominally spin at 100 RPM, this implies that these manoeuvres are actually a set of short bursts of the engines. Figure 25 shows what happens during a burst. At 100 RPM, there may be up to 100 bursts per minute. Despite this, it is possible in general to characterize all these manoeuvres as intantaneous manoeuvres in which all the ΔV is applied at the midpoint of the manoeuvre duration. This approach allows analysing the manoeuvres using the ordinary impulsive manoeuvre formulation.

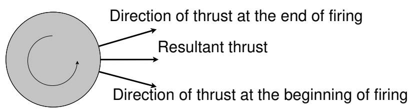

Figure 25. One burst in a tangential manoeuvre

After selected manoeuvres take place, the optical service performs a manoeuvre calibration. This calibration is performed by means of the BLS algorithm implemented in TRADE. The algorithm processes two weeks of orbit data, including tracks before the manoeuvre and the tracks taken the first night after the manoeuvre. The algorithm determines an augmented state vector that comprises the Cartesian state vector of the satellite at the epoch of the first track, and the three components of the ΔV vector at the manoeuvre centroid time. We assume as known the manoeuvre centroid time, and we consider as initial estimation the nominal manoeuvre ΔV as computed by the Eumetsat flight dynamics team.

In order to evaluate the manoeuvre calibration, we consider two figures of merit. On the first place, we define

#	Type	C	$\alpha(deg)$	$\|\Delta V\|(m/s)$
1	NSSK	1.0057	0.006770	45.428
2	NSSK	0.9930	3.38E-04	49.062
3	EWSK	0.9911	0.861103	0.2111
4	EWSK	0.9982	0.238523	0.1654
5	EWSK	0.9988	0.531437	0.2073
6	EWSK	1.0001	1.305736	0.2208
7	SLEW	1.0024	0.688026	0.0001
8	EWSK	0.9928	2.910313	0.1980
9	EWSK	1.0064	0.724250	0.2010
10	NSSK	1.0062	5.77E-03	42.964
11	EWSK	0.9987	0.118862	0.1588
12	SLEW	0.9607	1.06E+00	0.0439
13	EWSK	0.9959	0.713236	0.1943
14	EWSK	0.9969	9.42E-02	0.1599
15	EWSK	0.9971	0.513908	0.2311
16	EWSK	1.0006	0.215743	0.1879
17	EWSK	0.9964	0.493029	0.1728
18	EWSK	1.0076	1.527240	0.1643
19	EWSK	0.9988	0.306826	0.1764
20	SLEW	0.9795	1.008825	0.0795
21	EWSK	0.9957	0.144769	0.1457
22	NSSK	0.9779	5.18E-03	45.638
23	EWSK	0.9992	0.593425	0.1748
24	EWSK	1.0021	0.432838	0.1547
25	SLEW	0.9115	2.445671	0.0246
26	NSSK	0.9950	1.31E-02	3.8561
27	NSSK	0.9928	3.23E-02	41.537
28	EWSK	1.0150	0.218174	0.2163
29	EWSK	1.0898	23.38732	0.1477
30	EWSK	0.9956	0.570755	0.1563

Table 3. Results of manoeuvre calibration

the manoeuvre calibration factor (C) as:

$$C = \frac{|\Delta V|}{|\Delta V_{nominal}|} \tag{1}$$

We also evaluate the angular difference (α) between the nominal manoeuvre and the determined manoeuvre. Table 3 presents the results of all the manoeuvres that have been calibrated (notice that not all the manoeuvres that took place were calibrated). In general, we can see that the manoeuvre magnitude is always determined properly (on average, 0.997 and a standard deviation of 0.025). When observing the angular difference, we notice a relevant difference between the out-of-plane manoeuvres (NSSK) and the in-plane manoeuvres. The NSSK manoeuvres are two orders of magnitude larger than the in-plane manoeuvres, therefore, the determination of the angle is much less sensitive to noise, and this explains the difference between the values. In general, we can assume an angular difference of around 1 degree for in-plane manoeuvres and $1 \cdot 10^{-2}$ for out-of-plane manoeuvres.

The only outlier in this table is that in row 29*. This case is interesting because it illustrates how sensitive the orbit determination process is to the observation geometry. In this case, the manoeuvre took place at 27/10/2020 18:28 (UTC), and was performed by MSG2. The first manoeuvre calibration was attempted considering two weeks of data before the manoeuvre, and two tracks after it (this is in line with the data used in all other manoeuvres). The two tracks that were used in the first try were taken at 27/10/2020 18:45 (UTC) and 28/10/2020 18:07 (UTC). They were obtained this way because of bad weather conditions on the night of 27/10 that prevented us from taking observations later in that night. The other track was taken so that 2 tracks were provided 24 hours after the manoeuvre. Interestingly, the after-manoeuvre tracks were taken at roughly the same time of the day. As MSG2 is in a geosynchronous orbit, this means that the observation geometry was roughly identical for the three after-manoeuvre tracks. Doing the orbit determination with this case gave a very bad estimation for the manoeuvre: a size factor much larger than typical, and an angular difference of 23 degrees (one order of magnitude larger than expected). A quick analysis was carried out at Eumetsat and Deimos, and we quickly considered that the repeating geometry could be the cause of this. Additional observations were scheduled for the next night. One observation slot was taken, on purpose, at roughly the same time as the two previous days, while the other was taken at a different time. Table 4 summarises the results.

Case	Added tracks	C	$\alpha(deg)$
a	15 prior tracks + track @ 2020/10/27 18:45	1.1102	7.484416
b	previous tracks + track @ 2020/10/28 18:07	1.0898	23.38732
c	previous tracks + track @ 2020/10/29 19:06	1.0127	8.77874
d	previous tracks + track @ 2020/10/30 00:01	1.0007	0.62130

Table 4. Manoeuvre calibration for manoeuvre 29 and different track combinations

Fot starting the analysis, the case was executed considering just the first track that was obtained after the manoeuvre (Case a in table 4). This track was taken a few minutes after the manoeuvre took place, and the results are expectably bad, as the effects of the manoeuvre are hardly observable after the manoeuvre. Case b is the result that was obtained nominally, and is displayed as reference. Case c considers in total three tracks taken roughly at the same time of the night (and therefore, with roughly the same observational geometry). In this case, even when it has more observational data than all manoeuvres in table 3, the results are still noticeably worse than similar EWSK manoeuvres. Finally, case d includes an additional track taken at a different time of the night. We can see that this track alone is enough to make the solution become in line with other EWSK manoeuvres. It is worth noting that, in call the cases, the residuals of the BLS solution show a similar behaviour, with no apparent biases or other ill behaviours. Figure 26 summarises there results.

5.3. Statistics

The system has been operating since June 1 2018. Since that time, the following amount of data has been produced

- Total tracks: 4232
- Size in disk: 326 MB
- Total measurements: 3285776

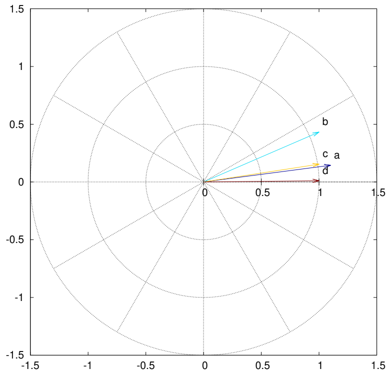

Figure 26. Polar plot of ΔVs determined in each case

- Measurements/track: 776
- Total observation time: 1246 hours
- Average observation time per track: 17.6 minutes

6. CONCLUSIONS

We presented a system that provides weekly optical observations and related products to geostationary operators. The provided data includes tracks, orbits (obtained by means of orbit determination applied on those tracks) and manoeuvre calibration. The system aimes at providing at the very least 2 tracks per week (with a minimum separation of at least 2 hours, even though it is preferable to take observations in different nights. These products provide enough quality to ensure orbit determination with a quality comparable to other, more costly systems. Manoeuvre calibration can also be performed exclusively with optical data. Overall, operators of GEO can obtain measurements of their satellites (and nearby satellites, if they want to), allowing them to compute precise orbit determination that can be used for their flight dynamics and/or conjunction avoidance systems. Additionally, they can obtain observations and perform orbit determination even in the case of a satellite malfunction.

ACKNOWLEDGMENTS

The authors want to acknowledge the work of the Deimos SSA team and the Eumetsat flight dynamics team for their support and availability to write this paper and during the operations that are described here. We are particularly grateful to Laura Pedrouzo (Deimos) and Antimo Damiano (Eumetsat).

REFERENCES

1. Domínguez-González, R. Nomen Torres, J., Oliviero, D., Sánchez-Ortiz, N. Klinc, M. Pessina, S., *Operational Orbit Determination for the Eumetsat GEO fleet based on optical observations*. (2018). ICATT 2018
2. Sánchez-Ortiz, N., Domínguez-González, R. Nomen Torres, J., Pessina, S., Klinc, M *Satellite flight dynamics activities supported by optical observations, lessons learnt from operational experience*. (2019). IAC 2019
3. Klinc, M., Pessina, S. *Optical tracking in support to routine operations and conjunctions analysis for the EUMETSAT geosynchronous fleet* (2015) 25th International Symposium on Space Flight Dynamics (ISSFD at DLR, Munich, Germany)
4. Klinc, M., Pessina, S. *Optical Tracking Extended Network in Support to Operational Flight Dynamics and Conjunction Analysis for Meteosat* (2017) 26th International Symposium on Space Flight Dynamics & 31st International Symposium on Space Technology and Science, ISTS-2017-d-156/ISSFD-2017-156
5. Klinc, M., Pessina, S., Sánchez-Ortiz, N. *Meteosat ranging antennas relocation: performance assessment and compensation using telescopes data service* (2019) 27th International Symposium on Space Flight Dynamics, ISSFD-2019
6. Pessina S., De Juana J. M., Fernandez J., Lazaro D., Righetti P. *Operational concepts refinement for the orbit determination of meteosat third generation* (2012) 23rd International Symposium on Space Flight Dynamics, ISSFD-2012
7. Schwer, A., Simon. D. *Meteosat 2nd Generation (MSG) - The unified propulsion system* (1997) Second European Propulsion Conference, ESA SP-398
8. Nomen Torres, J., Sánchez-Ortiz, N., Domínguez-González, R., Guijarro López, N., Quiles Ibernon, P. *Accurate Optical Observations of Space Objects in GEO and applicability to closer LEO regimes* (2017) 7th European Conference on Space Debris, ESA/ESOC, Darmstadt/Germany, 18 - 21 April 2017
9. G.J. Bierman *Factorization methods for discrete sequential estimation.* (1977)
10. William E. Wiesel *Modern orbit determination.* (2003)